ARMY RESEARCH LABORATORY

Modeling Graphene Contrast on Copper Surfaces Using Optical Microscopy

by Travis M Tumlin, Mark H Griep, Emil Sandoz-Rosado, and Shashi P Karna

ARL-TR-7134 **October 2014**

NOTICES

Disclaimers

Army Research Laboratory
Aberdeen Proving Ground, MD 21005-5069

ARL-TR-7134 **October 2014**

Modeling Graphene Contrast on Copper Surfaces Using Optical Microscopy

Travis M Tumlin, Mark H Griep, Emil Sandoz-Rosado, and Shashi P Karna
Weapons and Materials Research Directorate, ARL

Approved for public release; distribution is unlimited.

REPORT DOCUMENTATION PAGE

Form Approved
OMB No. 0704-0188

1. REPORT DATE *(DD-MM-YYYY)*	**2. REPORT TYPE**	**3. DATES COVERED (From - To)**
October 2014	Final	February 2014–July 2014

4. TITLE AND SUBTITLE
Modeling Graphene Contrast on Copper Surfaces Using Optical Microscopy

5a. CONTRACT NUMBER

5b. GRANT NUMBER

5c. PROGRAM ELEMENT NUMBER

6. AUTHOR(S)
Travis M Tumlin, Mark H Griep, Emil Sandoz-Rosado, and Shashi P Karna

5d. PROJECT NUMBER

5e. TASK NUMBER

5f. WORK UNIT NUMBER

7. PERFORMING ORGANIZATION NAME(S) AND ADDRESS(ES)
US Army Research Laboratory
ATTN: RDRL-WMM-A
Aberdeen Proving Ground, MD 21005-5069

8. PERFORMING ORGANIZATION REPORT NUMBER
ARL-TR-7134

9. SPONSORING/MONITORING AGENCY NAME(S) AND ADDRESS(ES)

10. SPONSOR/MONITOR'S ACRONYM(S)

11. SPONSOR/MONITOR'S REPORT NUMBER(S)

12. DISTRIBUTION/AVAILABILITY STATEMENT
Approved for public release; distribution is unlimited.

13. SUPPLEMENTARY NOTES

14. ABSTRACT
Since the discovery of graphene in 2004, extensive research has been performed to investigate uses for its excellent thermal, mechanical, and electrical properties. Top-down approaches such as mechanical exfoliation and chemical reduction along with bottom-up approaches such as chemical vapor deposition and molecular beam epitaxy are techniques that have been used to synthesize graphene and other 2-dimensional materials. Determining whether graphene has been successfully synthesized often requires transfer to a support substrate such as glass or SiO_2. During the transfer process, tears and impurities can be introduced, thus reducing the quality. In the present work, graphene has been imaged using confocal laser scanning microscopy and broadband optical microscopy. This technique allows graphene to be imaged directly on the copper substrate, thus eliminating the requirement for transfer. Atomic force microscopy was used to determine copper oxide thickness, and a Matlab model based on Fresnel theory was used to determine graphene contrast as a function of excitation wavelength. Different excitation wavelengths were used to determine the validity of the model over a wide range of the visible spectrum.

15. SUBJECT TERMS
graphene, contrast, optical modeling, Matlab, oxide growth

16. SECURITY CLASSIFICATION OF:			**17. LIMITATION OF ABSTRACT**	**18. NUMBER OF PAGES**	**19a. NAME OF RESPONSIBLE PERSON**
					Travis M Tumlin
a. REPORT	**b. ABSTRACT**	**c. THIS PAGE**			**19b. TELEPHONE NUMBER** (*Include area code*)
Unclassified	Unclassified	Unclassified	UU	20	410-306-0446

Standard Form 298 (Rev. 8/98)
Prescribed by ANSI Std. Z39.18

Contents

Lists of Figures **iv**

Acknowledgments **v**

1. Introduction and Background **1**

2. Materials and Methods **2**

2.1 Electropolishing of Copper Foils 2

2.2 CVD Synthesis of Graphene 2

2.3 CLSM and AFM Characterization 2

2.4 Broadband Optical Microscope Characterization 2

3. Results and Discussion **3**

3.1 Characterization of Graphene on Copper Using CLSM 3

3.2 Broadband Optical Characterization of Graphene Domains 4

3.3 Optical Modeling with Matlab 6

4. Summary and Conclusions **8**

5. References **9**

Distribution List **12**

List of Figures

Fig. 1 CLSM image of graphene domains on electropolished copper. Inset shows corresponding white light image. 3

Fig. 2 Narrow wavelength optical images of graphene domains on electropolished copper. Excitation wavelengths are A) 385 nm, B) 405 nm, C) 455 nm, and D) 530 nm 4

Fig. 3 Intensity profile for graphene domain with copper oxide as the background. Region of interest is outlined by the red square. 5

Fig. 4 Graphene contrast as a function of excitation wavelength 5

Fig. 5 AFM height (left) and phase (right) imaging. The inset on the height image shows the profile across the graphene domain. 6

Fig. 6 a) Graphene contrast modeling from Blake et al. compared with b) graphene contrast using in-house Matlab model 7

Fig. 7 Light interaction with copper oxide, graphene, and underlying copper surface 7

Fig. 8 Experimental contrast values compared with the Matlab contrast model 8

Acknowledgments

The authors would like to thank Kristopher Darling and Donovan Harris for allowing use of the confocal laser scanning microscope and broadband optical microscope.

INTENTIONALLY LEFT BLANK.

1. Introduction and Background

Since the discovery of graphene in 2004, extensive research has been performed to investigate uses for its excellent thermal, mechanical, and electrical properties.[1–4] Top-down approaches such as mechanical exfoliation and chemical reduction along with bottom-up approaches such as chemical vapor deposition (CVD) and molecular beam epitaxy are techniques that have been used to synthesize graphene and other 2-dimensional materials.[5,6] Nickel substrates played an important role in initial synthesis studies because of their close lattice match with graphene. The high carbon solubility, however, made it difficult to synthesize single monolayers because of surface segregation and subsequent precipitation of absorbed carbon species.[7–10] More recently, CVD of carbon precursors on copper substrates have risen to the forefront of graphene synthesis because of low cost and surface-mediated self-limited growth.[11–15] Characterizing the number of layers deposited can be a time-consuming process involving specialized techniques such as atomic force microscopy (AFM), scanning electron microscopy (SEM), transmission electron microscopy , Raman spectroscopy, and X-ray diffraction.[16–19] Several of these techniques, such as AFM and SEM, can be performed directly on the copper surface; however, further characterization of graphene usually requires transfer of the monolayer to another substrate such as glass or SiO_2.[20–22] Several early studies were done to characterize and model the number of graphene layers based on the contrast over the visible spectrum with an underlying dielectric substrate.[23–26] Again, a tedious transfer process was required to “see” the graphene. Another study focused on graphene’s contrast with dielectric, metal, and semiconductor substrates and enhancing that contrast by altering the thickness of polymethyl methacrylate deposited on top.[27] More recently, direct observation of graphene on copper using white light optical microscopy has been accomplished using a thermal annealing technique. This work allowed graphene to be imaged due to the increasing contrast between copper oxide and the copper protected by the grapheme.[28] Although the contrast imaging with graphene and copper oxide has been investigated, further work has yet to be completed on characterizing the changing contrast with respect to wavelength. The impact of oxide layer thickness and oxide layer growth on graphene contrast has also yet to be further characterized.

Herein, we report the observation of graphene on copper using a wide array of optical imaging techniques along with modeling the graphene contrast as a function of incident wavelength. Using a confocal laser scanning microscope (CLSM) and a broadband optical microscope, graphene has been imaged using different excitation wavelengths in the visible spectrum. The change in contrast over the visible spectrum further illustrates graphene’s unique optical properties. These optical methods allow quick observation of graphene domains and layers based on the contrast with the oxide layer. Graphene contrast was also modeled in Matlab using Fresnel theory equations. To verify the validity of the model, several wavelengths over the visible spectrum were used to experimentally quantify the contrast. The model is in good agreement with the experimental data suggesting that this model can be used for calculating graphene contrast on other metal catalyst substrates.

2. Materials and Methods

2.1 Electropolishing of Copper Foils

Copper foils (Alfa Aesar, 25 µm, 99.8%) were cleaned and degreased using an acetone, isopropyl alcohol, and milli-Q water rinse process prior to use. Reducing the copper surface roughness was carried out using a Struers Lectropol 5 automatic electropolishing unit. A mixture comprised of 330 mL deionized, distilled water, 167 mL ortho-phosphoric acid, 167 mL ethanol, 33 mL isopropyl alcohol, and 3.3 g of urea was used as the polishing electrolyte solution. Copper foils were prepared with an electropolished sample area of 5 cm^2. Electropolishing was performed across a potential of 8 V with a constant flow rate for the designated polishing time. After polishing, samples were rinsed with deionized, distilled water followed by a final rinse with isopropyl alcohol. Samples were then dried with a soft stream of nitrogen.

2.2 CVD Synthesis of Graphene

Graphene was synthesized using low-pressure chemical vapor deposition. The electropolished copper foils were transferred to a 1-inch-diameter tube furnace at 1,050 °C with pressure below 10E-6 Torr. Sample foils were annealed below 10E-6 Torr for 5 min under a 20-sccm argon and 10-sccm hydrogen gas mixture. Nucleated graphene growth is then achieved with the introduction of 5 sccm methane for 3 min.

2.3 CLSM and AFM Characterization

CLSM was performed using an Olympus OLS3100. Laser intensity was adjusted based on sample reflectance and 100× objectives were used as the primary means of imaging. A 405-nm laser was used as the excitation source. A Cypher SPM in noncontact mode was used for topography and phase imaging characterization.

2.4 Broadband Optical Microscope Characterization

Imaging over the visible spectrum was performed using a Zeiss Imager ZM2. Lamps with wavelengths of 385, 405, 455, and 530 nm were used as excitation sources.

3. Results and Discussion

3.1 Characterization of Graphene on Copper Using CLSM

Rapid optical characterization of graphene is dependent upon several factors. Most notably, the incoming light source plays a pivotal role in the contrast between the graphene and copper oxide. Figure 1 shows a CLSM image of graphene on copper using a 405-nm laser as the excitation source.

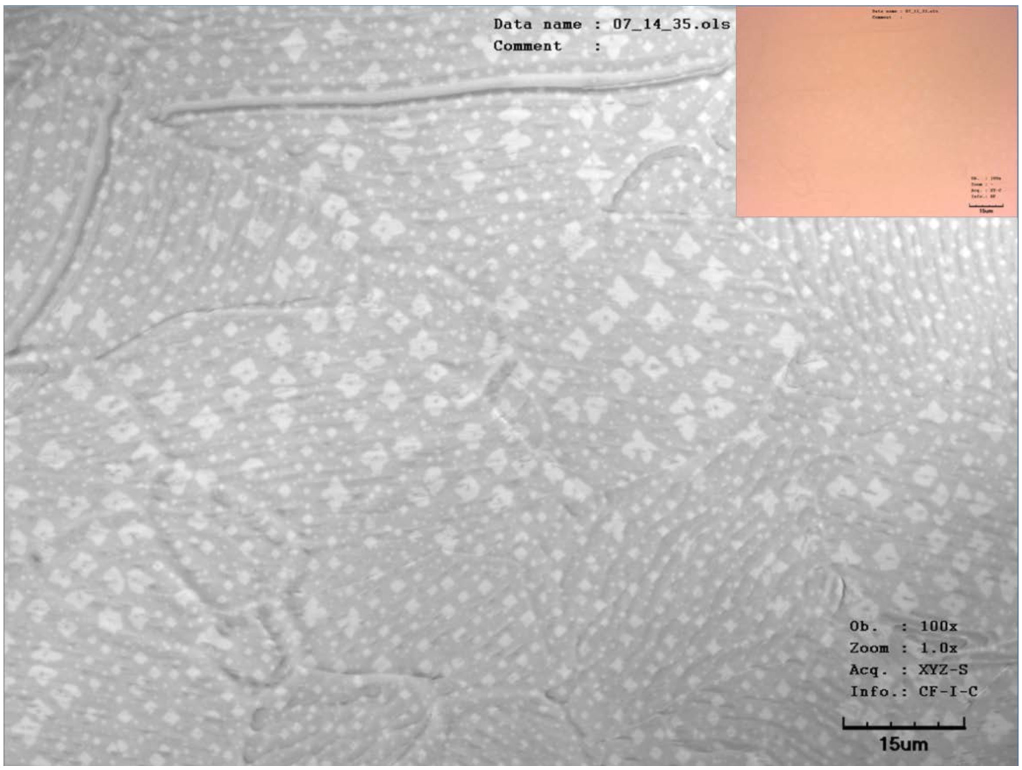

Fig. 1 CLSM image of graphene domains on electropolished copper. Inset shows corresponding white light image.

The graphene domains are clearly present showing an array of different geometries. Another important aspect to note is the inset image showing the graphene reflection with white light. The contrast with the broadband excitation is much lower as compared to the contrast with the narrowband 405-nm laser. This is due to the saturation effect that is seen with broadband imaging.

3.2 Broadband Optical Characterization of Graphene Domains

To further investigate the role of graphene contrast, narrowband LED light sources were used to map the contrast over the visible spectrum. Fig. 2 shows the graphene imaged with light wavelengths of 385, 405, 455, and 530 nm.

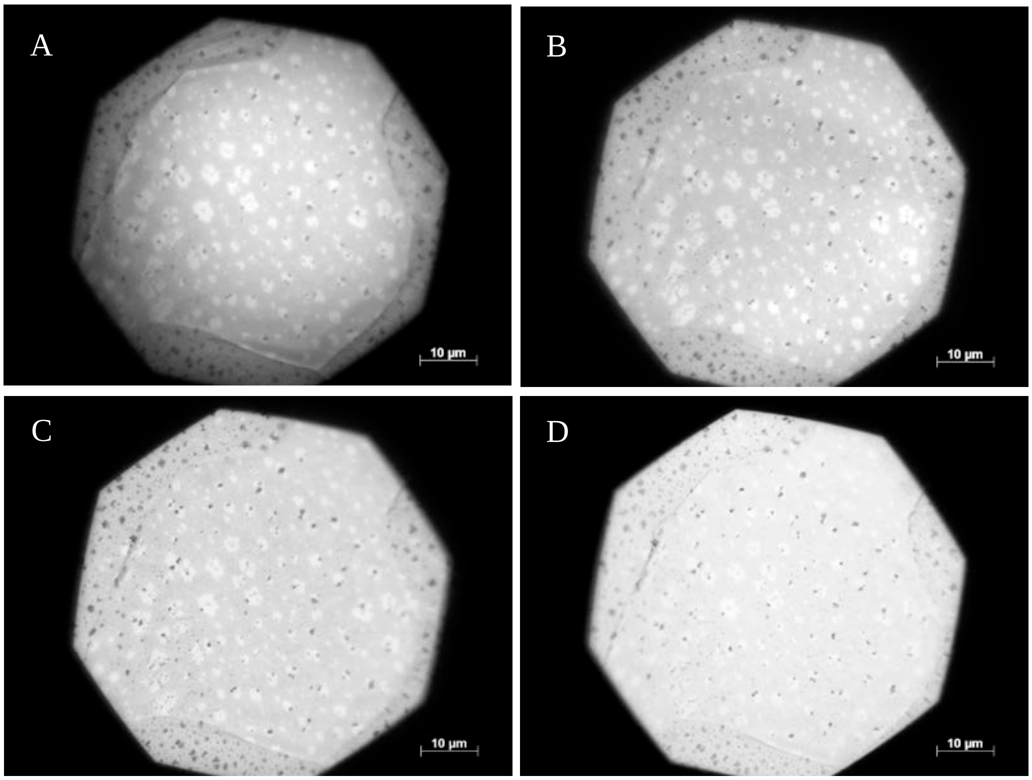

Fig. 2 Narrow wavelength optical images of graphene domains on electropolished copper. Excitation wavelengths are A) 385 nm, B) 405 nm, C) 455 nm, and D) 530 nm.

ImageJ, an image processing program, was used to determine the contrast between the graphene and copper oxide. Contrast was calculated using Eq. 1 where I represents the reflected intensity of the graphene and I_b represents the reflected intensity of the copper oxide.

$$C = \frac{I - I_b}{I_b} \,. \tag{1}$$

Intensity profiles were determined by placing a line over the region of interest. The values for intensity of the reflected light were calculated using gray number values. The intensity mapping over a graphene domain is shown in Fig. 3.

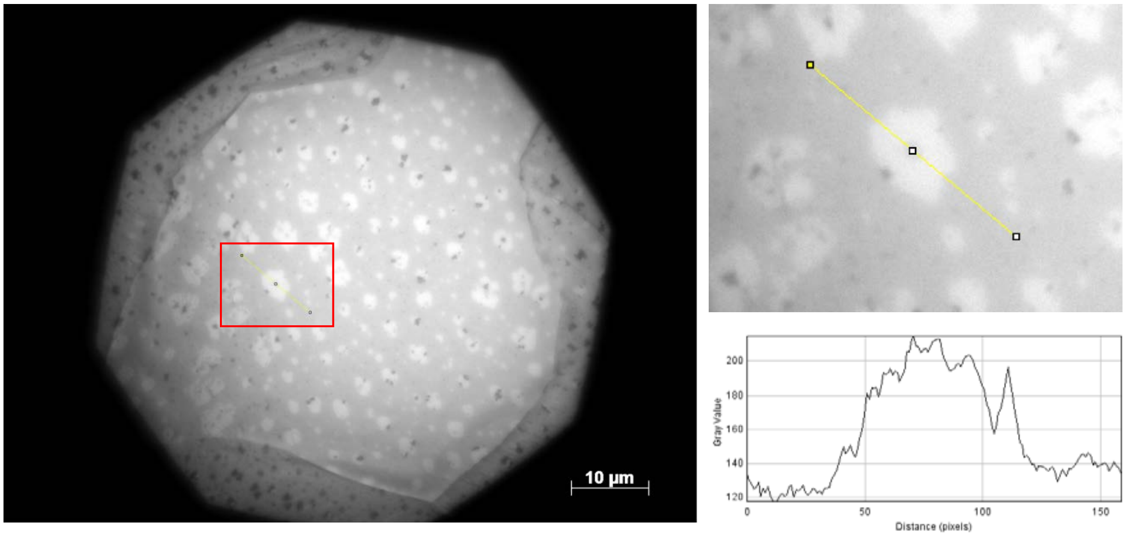

Fig. 3 Intensity profile for graphene domain with copper oxide as the background. Region of interest is outlined by the red square.

Since the background intensity of the reflected light is not constant over the entire image, a normalization process was used to even out each of the intensity profiles. The contrast of the graphene domains with respect to the copper oxide as a function of excitation wavelength is given in Fig. 4.

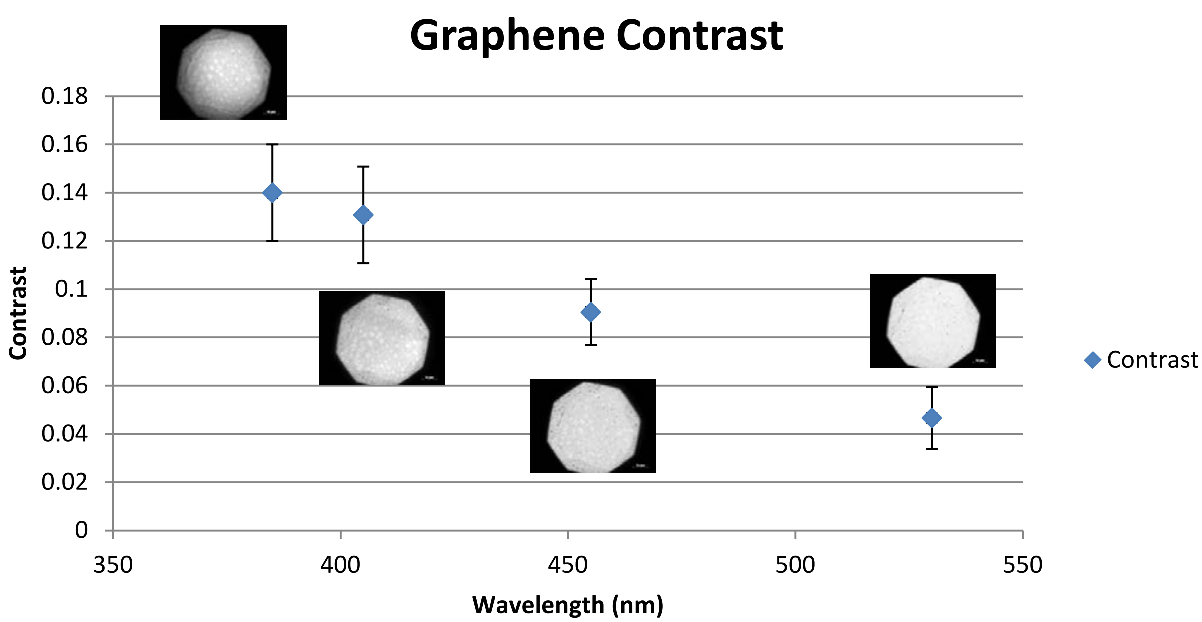

Fig. 4 Graphene contrast as a function of excitation wavelength

AFM was performed on the copper substrates to determine oxide layer thickness. Although the copper foil has surface striations as a result of the cold rolling process that makes height imaging difficult, the copper oxide thickness can be readily mapped using phase imaging. The height and phase image profiles are given in Fig. 5.

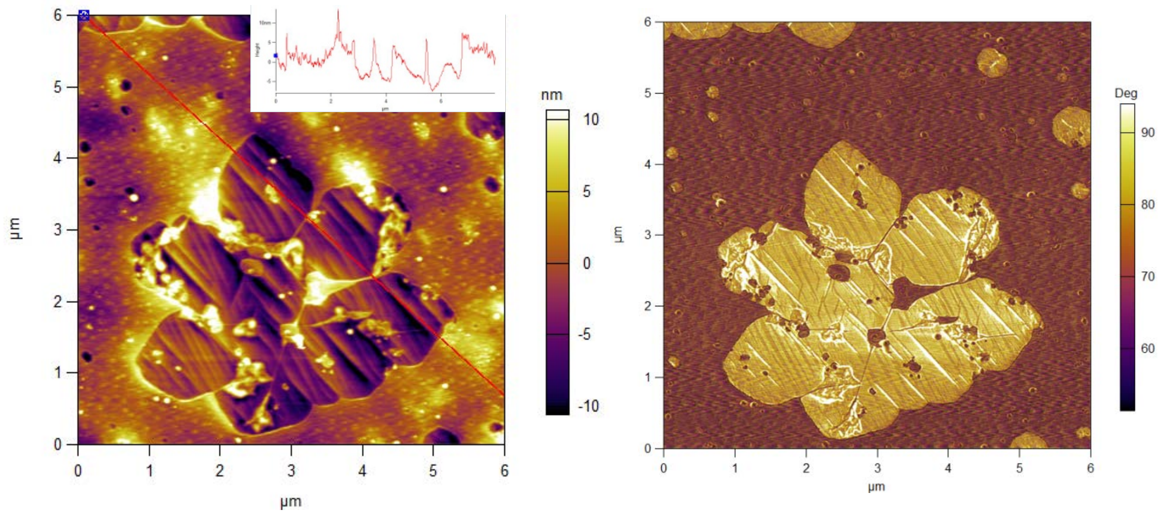

Fig. 5 AFM height (left) and phase (right) imaging. The inset on the height image shows the profile across the graphene domain.

AFM mapping confirmed the underlying copper surface that was covered by graphene was protected from oxidation while the unprotected copper surface was left to oxidize. It was found that the oxide thickness is approximately 10 nm.

3.3 Optical Modeling with Matlab

Because of graphene's unique optical properties, the contrast with the oxide layer can be modeled based on the Fresnel equations. Prior modeling has been done to show graphene's contrast with respect to an underlying dielectric substrate.[23–26] To verify Matlab's utility as a modeling tool in this study, a reflectance model was built to match what has been shown in literature. Fig. 6a shows graphene contrast with respect to wavelength and SiO_2 thickness from Blake et al.[23] In comparison, Fig. 6b shows the same graphene contrast calculations using an in-house Matlab model.

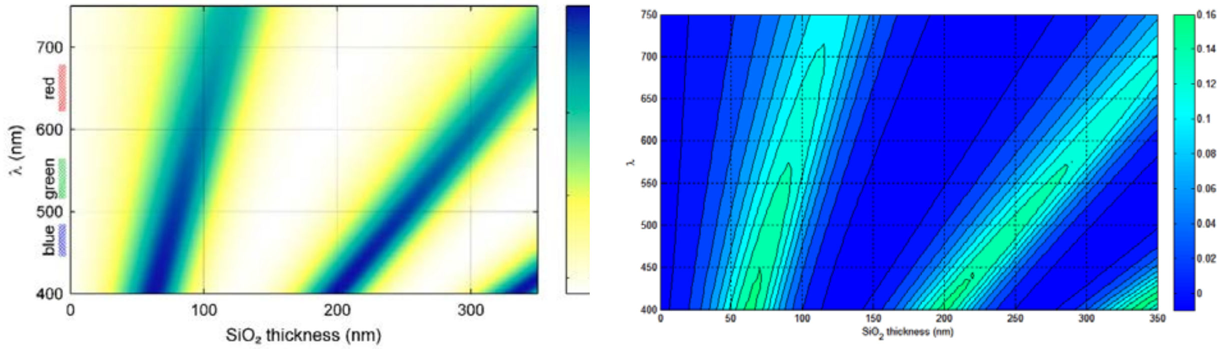

(a) **(b)**

Fig. 6 a) Graphene contrast modeling from Blake et al.[23] compared with b) graphene contrast using in-house Matlab model

To understand how light interacts with the graphene, copper oxide, and underlying copper substrate, it was first necessary to build a graphical template to understand the problem. Figure 7 shows the light interaction with the proposed model.

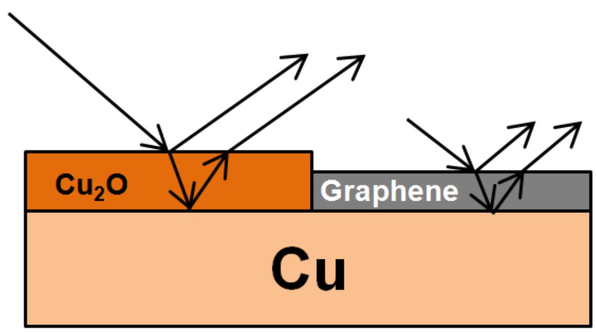

Fig. 7 Light interaction with copper oxide, graphene, and underlying copper surface

Eq. 2 shows the relationship for calculating the intensity of reflected light based on optical differences in the materials where Δ_1 is the phase shift and r_1 and r_2 represent the refractive indices of the materials.

$$R = \frac{{r_1}^2 + {r_1}^2 + 2r_1r_2\cos(\Delta_1)}{1 + {r_1}^2{r_2}^2 + 2r_1r_2\cos(\Delta_1)} \qquad (2)$$

By coupling Eq. 2 with Eq. 1, a value for contrast can then be determined from the modeled data. After determining the values for contrast from the modeled data, the model was compared with the contrast values that were determined experimentally. Figure 8 shows the model compared with the experimental data.

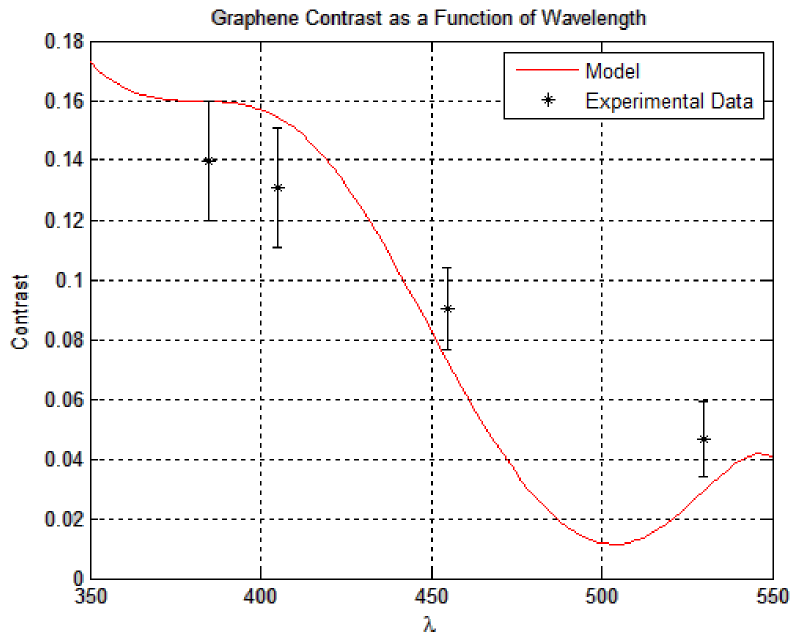

Fig. 8 Experimental contrast values compared with the Matlab contrast model

Figure 8 shows that the model is in good agreement with the experimental data. There is an overall decrease in contrast with reducing light energy, which infers that higher energy wavelengths in the visible spectrum are necessary for quality contrast imaging. Narrowband wavelengths are needed for contrast imaging due to the saturation effect that can be seen with broadband white light excitation.

4. Summary and Conclusions

In this report, graphene contrast with copper oxide has been calculated experimentally and modeled using Matlab. Using reflected light intensity and ImageJ processing software, contrast values over the visible spectrum were calculated based on the gray number value. A model was built in Matlab using reflection equations based on Fresnel theory to determine the change in contrast with respect to excitation wavelength. It was determined that incoming light energy plays a pivotal role in graphene contrast. As light energy is reduced, graphene contrast is also diminished, whereas higher energy wavelengths provide graphene with good optical contrast with respect to the copper oxide surface. Future work will focus on correlating oxide thickness to changes in contrast as well as modeling contrast as a function of the number of graphene layers.

5. References

1. Geim AK, Novoselov KS. The rise of graphene. Nature Materials. 2007;6(3):183–191.
2. Castro Neto AH, Guinea F, Peres NMR, Novoselov KS, Geim AK. The electronic properties of graphene. Reviews of Modern Physics. 2009;81(1):109–162.
3. Balandin, AA, Ghosh S, Bao W, Calizo I, Teweldebrhan D, Miao F, Lau CN. Superior thermal conductivity of single-layer graphene. Nano Letters. 2008;8(3):902–907.
4. Lee C, Wei X, Kysar JW, Hone J. Measurement of the elastic properties and intrinsic strength of monolayer graphene. Science. 2008;321(5887):385–388.
5. Moreau E, Godey S, Ferrer FJ, Vignaud D, Wallart X, Avila J, Asensio MC, Bournel F, Gallet J-J. Graphene growth by molecular beam epitaxy on the carbon-face of SiC. Applied Physics Letters. 2010;97(24):241907.
6. Reina A, Jia X, Ho J, Nezich D, Son H, Bulovic V, Dresselhaus MS, Kong J. Large area, few-layer graphene films on arbitrary substrates by chemical vapor deposition. Nano Letters. 2009;9(1):30–35.
7. Kim KS, Zhao Y, Jang H, Lee SY, Kim JM, Kim KS, Ahn JH, Kim P, Choi JY, Hong BH. Large-scale pattern growth of graphene films for stretchable transparent electrodes. Nature. 2009;457(7230):706–710.
8. Chae SJ, Güneş F, Kim KK, Kim ES, Han GH, Kim SM, Shin H-J, Yoon S-M, Choi J-Y, Park MH, Yang CW, Pribat D, Lee YH. Synthesis of large-area graphene layers on poly-nickel substrate by chemical vapor deposition: wrinkle formation. Advanced Materials. 2009;21(22):2328–2333.
9. De Arco LG, Yi Z; Kumar A, Chongwu Z. Synthesis, transfer, and devices of single-and few-layer graphene by chemical vapor deposition. Nanotechnology, IEEE Transactions. 2009;8(2):135–138.
10. Li X, Cai W, Colombo L, Ruoff RS. Evolution of graphene growth on Ni and Cu by carbon isotope labeling. Nano Letters. 2009;9(12):4268–4272.
11. Li X, Cai W, An J, Kim S, Nah J, Yang D, Piner R, Velamakanni A, Jung I, Tutuc E, Banerjee SK, Colombo L, Ruoff RS. Large-area synthesis of high-quality and uniform graphene films on copper foils. Science. 2009;324(5932):1312–1314.
12. Li X, Magnuson CW, Venugopal A, Tromp RM, Hannon JB, Vogel EM, Colombo L, Ruoff RS. Large-area graphene single crystals grown by low-pressure chemical vapor deposition of methane on copper. Journal of the American Chemical Society. 2011;133(9):2816–2819.

13. Guermoune A, Chari T, Popescu F, Sabri SS, Guillemette J, Skulason HS, Szkopek T, Siaj M. Chemical vapor deposition synthesis of graphene on copper with methanol, ethanol, and propanol precursors. Carbon. 2011;49(13):4204–4210.

14. Robertson AW, Warner JH. Hexagonal single crystal domains of few-layer graphene on copper foils. Nano Letters. 2011;11(3):1182–1189.

15. Yan Z, Lin J, Peng Z, Sun Z, Zhu Y, Li L, Xiang C, Samuel EL, Kittrell C, Tour JM. Toward the synthesis of wafer-scale single-crystal graphene on copper foils. ACS Nano. 2012;6(10):9110–9117.

16. Liu W, Li H, Xu C, Khatami Y, Banerjee K. Synthesis of high-quality monolayer and bilayer graphene on copper using chemical vapor deposition. Carbon. 2011;49(13):4122–4130.

17. Wang G, Yang J, Park J, Gou X, Wang B, Liu H, Yao J. Facile synthesis and characterization of graphene nanosheets. The Journal of Physical Chemistry C. 2008;112(22):8192–8195.

18. Ferrari AC, Meyer JC, Scardaci V, Casiraghi C, Lazzeri M, Mauri F, Piscanec S, Jiang D, Novoselov KS, Roth S, Geim AK. Raman spectrum of graphene and graphene layers. Physical Review Letters. 2006;97(18):187401.

19. Stankovich S, Dikin DA, Piner RD, Kohlhaas KA, Kleinhammes A, Jia Y, Wu Y, Nguyen ST, Ruoff RS. Synthesis of graphene-based nanosheets via chemical reduction of exfoliated graphite oxide. Carbon. 2007;45(7):1558–1565.

20. Wang Y, Miao C, Huang B-C, Zhu J, Liu W, Park Y, Xie Y-h, Woo JCS. Scalable synthesis of graphene on patterned Ni and transfer. IEEE Transactions on Electron Devices. 2010;57(12):3472–3476.

21. Regan W, Alem N, Alemán B, Geng B, Girit Ç, Maserati L, Wang F, Crommie M, Zettl A. A direct transfer of layer-area graphene. Applied Physics Letters. 2010;96(11):113102.

22. Kang, J, Shin D, Bae S, Hong BH. Graphene transfer: key for applications. Nanoscale. 2012;4(18):5527–5537.

23. Blake P, Hill EW, Castro Neto AH, Novoselov KS, Jiang D, Yang R, Booth TJ, Geim AK. Making graphene visible. Applied Physics Letters. 2007;91(6):063124.

24. Abergel DSL, Russell A, and Falko VI. Visibility of graphene flakes on a dielectric substrate. Applied Physics Letters. 2007;91(6):063125.

25. Roddaro S, Pingue P, Piazza V, Pellegrini V, Beltram F. The optical visibility of graphene: interference colors of ultrathin graphite on SiO_2. Nano Letters. 2007;7(9):2707–2710.

26. Jung I, Pelton M, Piner R, Dikin DA, Stankovich S, Watcharotone S, Hausner M, Ruoff RS. Simple approach for high-contrast optical imaging and characterization of graphene-based sheets. Nano Letters. 2007;7(12):3569–3575.

27. Teo G, Wang H, Wu Y, Guo Z, Zhang J, Ni Z, Shen Z. Visibility study of graphene multilayer structures. Journal of Applied Physics. 2008;103(12):124302.

28. Jia, C, Jiang J, Lin G, Guo X. Direct optical characterization of graphene growth and domains on growth substrates. Scientific Reports. 2012;2(707).

1 (PDF)	DEFENSE TECHNICAL INFORMATION CTR DTIC OCA
2 (PDF)	DIRECTOR US ARMY RESEARCH LAB RDRL CIO LL IMAL HRA MAIL & RECORDS MGMT
1 (PDF)	GOVT PRINTG OFC A MALHOTRA
5 (PDF)	DIR USARL RDRL WM S KARNA RDRL WMM A M GRIEP E SANDOZ-ROSADO J SANDS T TUMLIN